Since January 2020 Elsevier has created a COVID-19 resource centre with free information in English and Mandarin on the novel coronavirus COVID-19. The COVID-19 resource centre is hosted on Elsevier Connect, the company's public news and information website.

Biochimica et Biophysica Acta 1858 (2016) 1710–1721

Contents lists available at ScienceDirect

Biochimica et Biophysica Acta

journal homepage: www.elsevier.com/locate/bbamem

Viral channel forming proteins — How to assemble and depolarize lipid membranes in silico☆

Wolfgang B. Fischer *, Monoj Mon Kalita, Dieter Heermann [1]

[a] Institute of Biophotonics, School of Biomedical Science and Engineering, National Yang-Ming University, Taipei 112, Taiwan
[b] Biophotonics & Molecular Imaging Center (BMIRC), National Yang-Ming University, Taipei 112, Taiwan

ARTICLE INFO

Article history:
Received 17 November 2015
Received in revised form 14 January 2016
Accepted 18 January 2016
Available online 22 January 2016

Keywords:
Viral channel proteins
Protein structure
Protein assembly
Secondary structure prediction
Molecular dynamics simulations
Coarse grained simulations

ABSTRACT

Viral channel forming proteins (VCPs) have been discovered in the late 70s and are found in many viruses to date. Usually they are small and have to assemble to form channels which depolarize the lipid membrane of the host cells. Structural information is just about to emerge for just some of them. Thus, computational methods play a pivotal role in generating plausible structures which can be used in the drug development process. In this review the accumulation of structural data is introduced from a historical perspective. Computational performances and their predictive power are reported guided by biological questions such as the assembly, mechanism of function and drug–protein interaction of VCPs. An outlook of how coarse grained simulations can contribute to yet unexplored issues of these proteins is given. This article is part of a Special Issue entitled: Membrane Proteins edited by J.C. Gumbart and Sergei Noskov.

1. Introduction

Bridging computation and experiments implies that there are two independent worlds each of which delivers information by itself but mutually supports the overall investigations on a subject, here a protein. Computational results help to predict and need verification from experiments. It is the view however, that based on high quality computational developments, computational modeling should also be seen as a source for delivering of smart 'suggestions' which need to be 'matched' with experiments.

Abbreviations: AMA, amantadine; BFM, bond fluctuation method; BST-2, bone marrow stromal cell antigen 2; CD, circular dichroism; CGMD, coarse-grained molecular dynamics; ClyA, cytolysin A; DHPC, dihexanoylphosphocholine; DPC, dodecylphosphocholine; *E. coli*, *Escherichia coli*; EM, electron microscopy; ff, force field; FTIR, Fourier transform infrared; GT, genotype; HCV, hepatitis C virus; HepG2, hepatocellular carcinoma cell line 2; HIV, human immunodeficiency virus; HMA, hexamethylene amiloride; HPV, human papillomavirus; MscL, large-conductance mechanosensitive channel; MS-EVB2, multi state empirical valence bond model 2; nAChR, nicotinic acetylcholine receptor; NMR, nuclear magnetic resonance; NN-DNJ, N-nonyl-deoxynojirimycin; PDB, protein data bank; PMF, potential of mean force; REMD, replica exchange molecular dynamics; RIM, rimantadine; RMSD, root mean square deviation; RyR2, ryanodine receptor 2; SARS-CoV, sever acute respiratory syndrome coronavirus; SPPS, solid-phase peptide synthesis; ssNMR, solid state NMR; TCP, thermodynamic cycle perturbation method; TFE, trifluoroethanol; TMD, transmembrane domain; VCP, viral channel forming protein; Vpu, viral protein U.

☆ This article is part of a Special Issue entitled: Membrane Proteins edited by J.C. Gumbart and Sergei Noskov.

* Corresponding author.
E-mail address: wfischer@ym.edu.tw (W.B. Fischer).
[1] Institute for Theoretical Physics, University of Heidelberg, Germany.

1.1. Historical perspective

Evidence for the existence of proteins encoded by viruses which alter membrane permeability has been reported for the first time in the late 70s [1,2]. It had been found that synthesis of host proteins in cells invaded by viruses is lowered in order to allow viral protein synthesis to occur. This finding has been called the 'shut-off phenomenon'. The cause of this phenomenon was attributed to 'coat proteins' causing an alteration of ion gradients within the infected cell which gave rise to speak about a 'membrane leakage-model': proteins must exist which form 'small pores in the lipid bilayer through which ions could diffuse freely' [1].

In the 90s, proteins which alter membrane permeability were identified for a series of viruses such as 2B and 3A of polio virus [3], 6K protein of Semliki Forest virus [4], M2 of influenza A [5,6] and Vpu of HIV-1 [7,8]. Since then the number of identified and proposed channel proteins has risen (see reviews [9–15]). Identification of altered membrane permeability by the VCPs is mostly based on in vitro experiments. An immediate correlation of protein activity within the cell is unambiguously established only for very few of them.

The outcome of most of the in vitro studies is that the channels formed by the VCPs lack sophisticated gating behavior and a high selectivity. All together it seems that some of the VCPs form pores which are, to some extent, selective similar to the host ion channels. Other VCPs show characteristics like toxins by simply enabling unselective permeability for even small molecules. Experimental data support a channel-pore dualism [16]. Based on these facts the VCPs are evidently termed

http://dx.doi.org/10.1016/j.bbamem.2016.01.018
0005-2736/

Table 1
Timeline of the emergence of structural information of the VCPs. F = FTIR, H = hypothesized, CD = circular dichroism, N = NMR, E = EM, X = X-ray, D = drug, fl = full length protein, sgl = single TMD.

year	85	86	87	88	89	90	91	92	93	94	95	96	97	98	99	00	01	02	03	04	05	06	07	08	09	10	11	12	13	14	15
M2 TMD	H			H				CD					N		F									X		D					
																								D							
Vpu cyto											N	N	N																		
TMD				H											N/F	N												D			
P7 fl										H		H							E			E			E	N			N	N	
																													D		
sgl																										N					
2B												H																			
E5				H						F								CD													

as viroporins. Usually membrane proteins with beta barrel motif for the transmembrane domain are termed as 'porins'. However, as shown below, such a motif is not reported for any of the VCPs so far.

Structural information about the VCPs is gradually emerging due to the fact that they are small and embedded within the lipid membrane [12] (Table 1). Spear headers in respect to availability of structural information are M2 of influenza A and Vpu of HIV-1 most recently followed by p7 of hepatitis C virus. This feature is in line with the importance of the VCPs being potential drug targets. Nevertheless most of the structural information is limited to the TMDs of the VCPs and in the case of Vpu it includes also solely the cytoplasmic domain. Most recently a synthetic peptide corresponding to the extramembrane N terminal side of M2 has been crystallized in contact with a monoclonal antibody [17]. The structure can be regarded as a good approximation to the 'in vivo' structure of M2.

For many of the VCPs, channel function is reported to be non-essential [15]. In the case of Vpu it is not even identified whether a channel function is needed at all in the infectivity cycle of the virus [18].

As a drug target, the VCPs are just emerging as potential candidates since for many viruses they are not essential for survival. Therefore most of these proteins are classified as 'auxiliary' proteins. M2 from influenza A, the first VCP to be detected, has also been the target for the very first ever developed antivirals. At this moment only a hand full of other drugs are tested against VCPs. One drug is explored in clinical trials to combat HCV/HIV-1 targeting p7/Vpu. Difficulties in getting structure information, an essential prerequisite for effective drug development, foster the low attractiveness in drug development.

Another facet in the function of these viral channel forming proteins is the fact that, starting with Vpu of HIV, host factors are identified, with which the VCPs interact to steer the cells towards improved viral replication [19]. Recently a VCP of human papillomavirus, E5, has entered the league of VCPs [20]. Until then E5 had been identified as to interact with a series of host factors. Also p7 of HCV is proposed to interact with host proteins whereas experimental data identify large scale interactions with other membrane proteins of its own genome. At this moment these interactions may open a route for the development of conceptually novel drugs targeting the VCPs [21].

Low selectivity together with dual functionality, as VCP and steering molecule, supports the rather obscure characterization of these types of biomolecules being plastic and highly dynamic multi-tasking membrane proteins.

A solution to the bottle neck imposed by structural virology and the fuzziness of their mechanical behavior is to enroll into computational approaches which help to answer academic questions and support the drug development process. The intention of this review is to focus on computational modeling as the source of information.

1.2. Structural information from experimental techniques — a survey

At this stage it is the intention to survey and illuminate the structural (Table 2) and computational research on the VCPs. For more detailed information about the molecular biological features the reader may be referred to excellent reviews available in the literature, e.g. [13,15]. Structural information forms the cradle of computational modeling.

The very first structural information about a VCP was given for a synthetic peptide corresponding to the TMD of M2 of influenza A using CD spectroscopy [22] (Table 1). A helical motif has been identified. Solid state NMR spectroscopic experiments, also based on synthetic peptides corresponding to the TMD of M2, proposed a defined tilt of the peptide and left-handedness of the putative tetrameric bundle [23]. Also FTIR spectroscopic measurements on similar peptides supported the tetrameric assembly [24]. In a series of solid state NMR spectroscopic investigations using synthetic constructs [25] or expressed peptides [26,27] precise orientations of side chains of tryptophan and the essential histidines were obtained and an elaborate model of the mechanics of proton movement was established [25–27].

The M2 protein in its tetrameric state was also identified using solution NMR spectroscopy [28] (Fig. 1). At the same time X-ray spectroscopic data were available [29] (Fig. 1). All data sets reveal the left-handed nature of the helical assembly and also support the notation that the TMDs can form the assembly independent of the extramembrane domains. And following up on this, a full protein structure of M2 neither in its monomeric nor in its tetrameric form is available.

In a series of structural experiments the location of drugs such as amantadine [30] (2KQT), [29] (3C9J) and rimantadine [28] (2RLF), [31] (2LJC) and other drugs, e.g. amantadine derivatives [32] (2LY0), and [33] (2MUV) has been investigated.

The next VCP in line is Vpu of HIV-1 for which structural information has become available. Its cytoplasmic domain has been expressed in *E. coli* [34] or synthesized [35,36] and used in CD spectroscopic and solution NMR experiments. Later the structure was refined by expressed *E. coli* protein reconstituted into detergent micelles of DPC [37] (Fig. 1). The structure represents an improvement since in the studies reported earlier the VCPs have been resolved either in TFE containing solution [35,36] or in buffer of high salt concentration (500 mM sodium sulfate) [34]. What all structural studies have

Table 2
Structural features of the VCPs placed in the PDB (www.rcsb.org) denoted by their PDB ID. 'NED' and 'CED' stand for 'N-' and 'C-terminal extramembrane domain'.

Protein	N-terminal	TMD	C-terminal	Technique
Vpu		monomer 2GOF and 2GOH [129] monomer 2JPX (mutant A18H [130]) monomer 1PJE [42] tetramer 1PI8 and pentamer 1PI7 [42]		ssNMR
				for structural information not available in the PDB see [39, 43]; FTIR [89]
			1VPU [34] 2K7Y [37] 2 N29 [45]	solution NMR
				for structural information not available in the PDB see [35]
	Full length unphosphorylated Vpu 2 N28 [45]			Solution NMR,
P7	No	TMD2: 2K8J [49]	No CED	solution NMR
	NED	Monomer: 3ZD0 [51], 2MTS [50]		solution NMR
		Hexameric bundle: 2M6X [52]		solution NMR
				for structural information not available in the PDB see [47, 48] bundle from EM: [53-55]
M2		Tetramer: - 2KWX V27A mutant [131]		solution NMR
		- 2KQT [30] + AMA		ssNMR and computer modeling
		- 3LBW [115]		crystal structure
		- 2RLF [28] + RIM		solution NMR
		- 3C9J, 3BKD [29] + (3C9J + AMA)		crystal structure
		- 2KIH S31N mutant [132]		solution NMR
		- 2LY0 S31N [32] + AMA-Deriv		solution NMR
		- 2MUV, 2MUW [33] + AMA Deriv		solution NMR
		- 2KIX influenza B [133]		solution NMR
		- 2LJB, 2LJC AM2-BM2 chimera [31]		solution NMR
		- 2KAD [134]		ss NMR
		- 2H95 [135]		ss NMR
		- 2L0J [136]		ss NMR
		- 1NYJ [25]		ss NMR
		Monomer - 1MP6 [137]		ss NMR

in common is the fact that the two serines at positions 52 and 56 are not phosphorylated as found in vivo. NMR spectroscopic investigations of the cytoplasmic domain, Vpu_{39-81}, when phosphorylated and recorded in the presence of DPC reveal no major structural changes compared to the unphosphorylated form [37,38]. In contrast, NMR spectroscopic investigations with a synthetically derived shorter cytoplasmic fragment, Vpu_{41-62}, recorded in TFE containing solution indicate a structural change of the phosphorylated Vpu_{41-62} towards its C-terminal side [39].

Solid state NMR spectroscopic data of the TMD of Vpu identified a helical motif for this part of the protein [40,41]. The TMD is comprised of two segments connected by some residues, e.g. Ile-17, which are showing large dynamics in the spectra [42]. In addition ssNMR reveals that the second helix is aligning along the membrane surface [43,44]. The oligomeric state of peptides corresponding to the TMD of Vpu is proposed to be tetra- and pentameric [42]. Most recently, a full length unphosphorylated Vpu structure is reported from solution NMR spectroscopy (PDB ID: 2N28) when reconstituted into DHPC (1,2-dihexanoyl-sn-glycero-3-phosphatidylcholine) [45] (Fig. 1). In this structure the cytoplasmic domain is found in a U-shape form, identified to be highly flexible and the third helix being positioned within the lipid membrane.

The overall structure of Vpu is controversial in respect to the cytoplasmic domain. The structural models show the domain in either a more compact [34,37,38] or a more elongated structure [35,45]. In the latter case, the third helix of Vpu is proposed to be flexible and is positioned either above [35] or within the lipid membrane [45].

Structural information with any drug is not available at the PDB. However, contact amino acids between the TMDs of Vpu and BST-2 are mapped using solid state NMR spectroscopy [46].

Overall, the structure of Vpu is that of a short unstructured N terminus, a helical TMD, and a cytoplasmic part composed of a helix-turn-helix motif with the first helix of this motif supposed to be membrane attached. The oligomeric state based on structural data may not exceed a pentamer.

Polytopic topology of p7 of HCV with two TMDs has been confirmed using solid state NMR spectroscopy [47,48] and solution NMR spectroscopy [49–51] (Fig. 1). These studies reflect structural information at the monomeric level using sequences of GT 1b either expressed by *E. coli* [47,48,50,51] or derived from SPPS [49]. Protein p7 can be seen to consist of two membrane spanning segments. One of the segments is fragmented into smaller helical units which are separated by a very short dynamical unit [47–50]. A bundle structure consisting of six monomers could be resolved by solution NMR spectroscopy of a viral ion channel for the first time using the amino acid sequence of p7 of GT 5a with some mutations at non-conserved positions to improve protein stability expressed in *E. coli* [52]. The structure of this bundle does not fit into the picture of somehow aligned monomeric units with antiparallel aligned TMDs but rather illuminates an intercalated clamp-like assembly in which one monomer connects with the fourth monomer (i + 3 motif). The overall architecture is that of a funnel with a larger loop-like region than proposed by aforementioned models. Thus, in the case of p7 it seems that GT specificity of the sequence may result in GT specific structures.

Features of p7 bundles have been derived using transmission EM. Cross-linked p7 of GT 1b expressed in HepG2 cells assembles into hexamers [53]. The same p7 strain expressed with a FLAG-tag expressed in *E. coli* delivers a heptameric assembly [54]. In a more recent study, p7 of GT 2a obtained from SPPS appears as a 'flower-shaped' bundle [55]. The orientation of the antiparallel aligned monomer within the shape of the EM density map is proposed with the two termini towards the wider section of the density map.

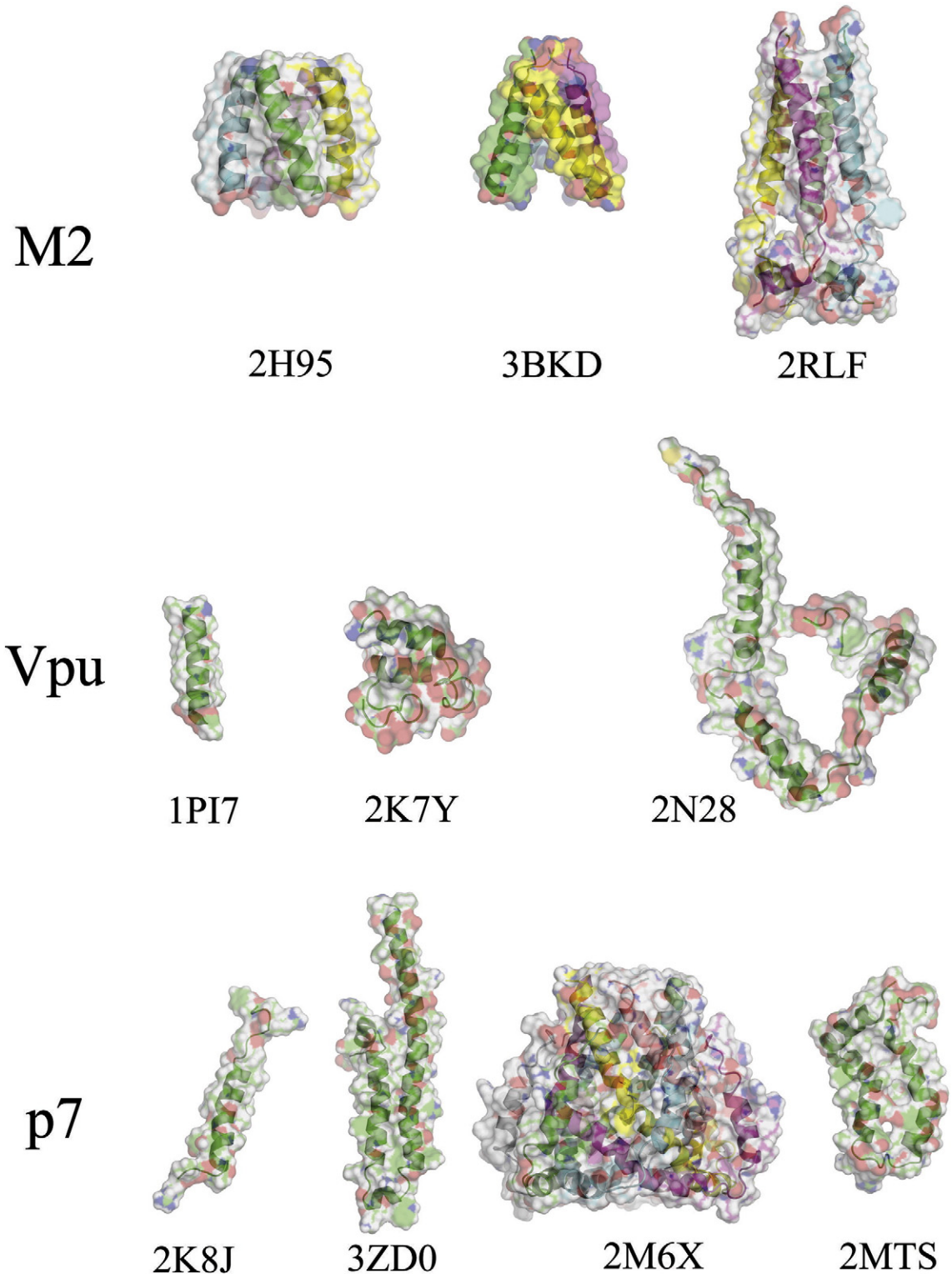

Fig. 1. Available structural models of VCPs M2 of influenza A (PDB IDs: 2H95ss [138], 3BKD [29], 2RLFsol [28]), Vpu of HIV-1 (PDB IDs: 1PI7 [42], 2K7Y [37]) and p7 of HCV (PDB IDs: 2K8J [49], 3ZD0 [51], 2M6X [52], 2MTS [50]) in the PDB. Structure 3BKD is the only structure derived from X-ray crystallography.

Investigations on ligand–protein p7 interactions are based on solid state NMR spectroscopy (amantadine, *N*N-DNJ, HMA) [50] and solution NMR spectroscopy (amantadine) [52].

Protein p7 seems to adopt GT specific structural features in respect to its tertiary fold and possibly also to its quaternary structure. It is most likely that the protein can be modeled as a hexameric bundle. It is so far the only VCP for which a bundle structure is available for its full length protein.

Experimental studies on E5 of HPV have delivered controversial results. While an early study using FTIR spectroscopy proposes high helical content of peptides including the putative TMD sequences [56], a CD spectroscopy investigation also on peptides corresponding to the

identified TMDs results to the presence of considerable β-sheet contents of the peptides [57]. In both experiments peptides have been dissolved in TFE.

2. Bridging from experiments to structure via computation

2.1. Obtaining structure from computation

Experiments form the ultimate source of structural information. Nevertheless, in silico approaches can also be pursued to derive relevant structural information especially when experimental data recording remains difficult. A basic necessity for any computational technique is the primary structure of the relevant protein which can only be achieved by experiments. With the primary structure at hand alignment programs can be fed to derive information about how much other organisms use the same sequence for the same purpose.

One of the earliest predictions of secondary structural elements, especially helices is reported in 1965 [58]. The amino acid sequence of myoglobin and hemoglobin is analyzed for patterns which are responsible for helices to end, when comparing with information from crystal structure. Similarly, prediction programs are available especially to predict TMDs of the VCPs (see. e.g. [59]).

Prediction programs in connection with the VCPs have been used to identify TMDs when novel proteins are identified. For the bitopic proteins M2 of influenza A [60] and Vpu of HIV [61] the Kyte–Doolittle index of hydrophobicity [62] has been applied. Similarly for the E5 protein of HPV the same index has been adopted to mention a trimodal hydrophobic structure [63]. Polytopic protein p7 of HCV with 2 TMD has been suggested to be so based on experimental data of cleavage products [64] and predicted [65] on the bases of hydrophobicity analysis using the Hopp–Wood indices [66]. The two TMDs of 2B from polio/coxsackie virus are proposed [67] by calculating the mean hydrophobic moment and hydrophobicity of an 11-residue window according to [68].

2.2. From primary to secondary structure

In the case of M2 of influenza A, the first structural model of the tetrameric bundle with helical motif for the TMDs is proposed on the bases on the amphiphilic character of the TMD and its sidedness as well as escape mutations identified within the hydrophilic side of the proposed helical motif [69]. Since the proposal has quickly been experimentally confirmed [22], early computational modeling data could rely on this information [70].

In analogy to the findings for M2, literally ahead of experimental verification in 1999 [40], the secondary structure of Vpu was assumed to be helical and structure based MD simulations performed [71]. In the need of assembling to form an ion conducting channel a helical motif has been assumed as the most likely structural motif. One of the earliest structural predictions was made for the cytoplasmic domain of Vpu suggesting a helix-turn-helix motif by using 'in-house' developed software [72]. In the case of p7, secondary structure prediction programs for membrane proteins form the bases for definition of the helical motif [73] prior to experimental verification [47,49] (Fig. 2).

Currently, there are several bundle models available based on the knowledge of the primary sequence of the TMD and the oligomeric state of the protein in its putative functional form. The detected two TMDs of 2B of polio/coxsackie virus have been immediately interpreted as to adopt a helical motif based on sided amphiphilicity in a helical projection [67,74]. Computer based structural models do exist waiting for experimental verification [75]. Protein 3a of SARS-CoV has been identified [76] and consequently modeled in a tetrameric form with 3 TMDs forming the monomer [77].

Despite earlier controversial structural data, E5 of HPV is modeled with its three TMD in a helical motif as a hexamer on the basis on topology prediction programs [20]. The hexameric bundle is used in a drug screening experiment.

2.3. From secondary to tertiary and quaternary structure

Once the secondary structure of the viral proteins is identified, the next steps depend on the topology of the protein. In the case of bitopic proteins, the helices can be consequently aligned into a barrel stave model (Fig. 2). In the case of polytopic proteins, the helices need to be arranged into a monomeric model prior to assembling into a bundle model.

As described by the barrel-stave model a pore in a membrane is due to the assembly of the peptides into a cyclic arrangement held together by inter-peptide interactions [78,79]. Especially in the case of bitopic VCPs it is tempting to assume a similar arrangement of the bundle. A competing model for pore formation is the toroidal model [78,79] in which the peptides form a pore 'together with the lipids'. Such a pore would have lipids facing the lumen and it is anticipated that this kind of pore should not exhibit high selectivity as well as eventually sophisticated gating behavior of the VCPs.

The preference for the former arrangement of the VCPs is based on early channel recording data on M2 of influenza A [5,80] and Vpu of HIV-1 [7,8] which show distinct conductance levels. Early modeling of the assembly of the TMDs to form a pore and work thereafter has followed this concept [71,81]. The overall weak ion selectivity found for any of these VCPs may not fully exclude the toroidal model. Modeling of the toroidal feature is still a challenge with many ambiguities.

Early assembly protocols have used ideal helical structures, copied them around a central axis and performed an assessment of the bundle structure based on the hydrophobicity potential [70] or RMSD after short energy minimization steps [82]. This protocol forms the basis for the assembly of bitopic VCPs such as Vpu [71,83], M2 of influenza A [70,81,84] and NB of influenza B [85]. Conformational search was limited on the bases of knowledge-based architectural constrains such as that hydrophilic residues within the hydrophobic slab should point into the center of a putative pore. The first model of the polytopic p7 with two TMDs was generated by using a full 360° rotational search of the two TMDs to form the monomer and the consequent 6 monomers arranged around a pseudo six-fold axis to form the hexamer according to the above mentioned protocol [73]. In addition available docking software, e.g. DOT and GRAMM, has been used to cross-check the results.

Extended protocols have been developed thereafter based on a fine grained screening of conformational space when assembling the helices in a bundle like arrangement [86]. The concept of the screening is that the Cα atoms are moved during the individual steps screening distance, rotation and tilt. Side chains are imposed at each position and after short energy minimization the potential energy of the respective structure is obtained using the AMBER96 force field. Scoring can be done by monitoring the energy landscape and picking the structure with the lowest energy.

The protocol is now extended to screen conformational space also of heterologous TMD assemblies as needed when generating the monomeric unit of polytopic VCPs [77]. With this protocol, models of p7

Fig. 2. Flow-chart of the computational modeling of bitopic and polytopic membrane proteins. In the first step the TMDs of are predicted by using secondary structure prediction programs (e.g. MemBrain [139], TMPRED [140], DAS [141], TMHMM [142], TOPPRED2 [143], SOSUI [144], HMMTOP [145], JPRED3 [146], PHDtm [147]). The results of the predicting helical motifs (indicated as "*") can be aligned to decide the length of the TMD used in the follow-up protocol. The TMDs can then be modeled as helices. In this case, the two TMDs, green and red, are shown for p7 of HCV. The dark blue ends are non-helical extramembrane regions. The loop region, connecting the two TMDs is drawn in black. The two individual TMDs will be docked by screening distance, tilt and rotational angles using a force field based scoring function. In a consecutive step, the polytopic monomer then needs to be docked to form the respective oligomer.

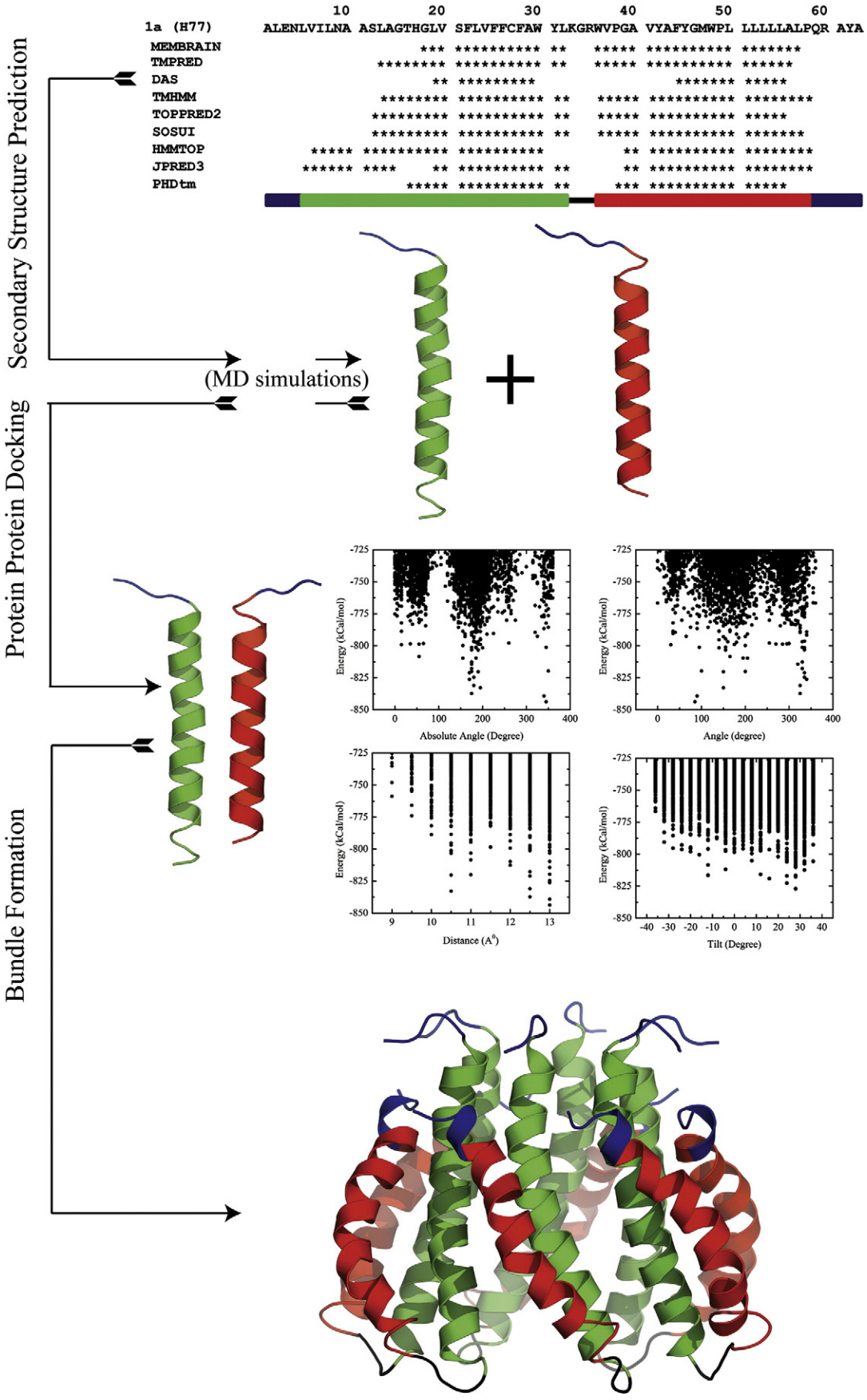
Secondary Structure Prediction
Protein Protein Docking
Bundle Formation
(MD simulations)
1a (H77)
MEMBRAIN
TMPRED
DAS
TMHMM
TOPPRED2
SOSUI
HMMTOP
JPRED3
PHDtm
Energy (kCal/mol)
Absolute Angle (Degree)
Angle (degree)
Distance (A°)
Tilt (Degree)

[87,88] as well as models of 3a of SARS-CoV which contains three TMDs per monomer [77] have been generated.

In another protocol, putative bundle structures of M2 of influenza A and Vpu of HIV-1 have been assessed by comparison of tilt angles with values derived from FTIR spectroscopy [24,89]. Energy minimization at each position have been done by short MD simulations. The search space however, has been be limited based on constraints derived from the experimental data.

The principles of prepositioning ideal helices around a central axis to generate a bundle based on known architectures are generally used if knowledge-based architectural constraints allow to do so as in the case of Vpu [90,91]. These bundle models are then used in classical [90] or REMD simulations [91] to address mechanical features. In other studies, e.g. on p7, the tertiary structure was modeled along these lines but the structure of the monomer was based on experimental (NMR) data [92].

Generating the models using a fine grained conformational search protocol in combination with force field based scoring is an established route to generate first hand models of assembled VCPs. In the case of M2 as well as Vpu, experimental data from NMR spectroscopy support the parallel alignment of the helices. In the case of p7 some controversies have arisen. While solid state NMR data confirm the modeled data using the described protocol, recent solution NMR spectroscopic data of p7 identify a bundle architecture which would be difficult to model using the protocols mentioned so far.

2.4. Computational derived models and their matches with experimental data

A series of models of tetrameric M2 of influenza A have been generated by in silico methods and used in MD simulations. [84,93]. In these models, hydrophilic residues of M2 including the important residue His-17 align at one side of the helix so that the tetramer adopts a plausible pore architecture. Comparison of the bundles of M2 with experimental data shows very good matches [94].

In the case of Vpu of HIV-1, computational assembly studies deliver a putative hydrophobic pore independent of the oligomeric state [42,95–97]. Such conformation matches experimental data. However, an architecture like this is somehow in conflict with the current idea of a pore architecture of ion channels. Regarding other structural features, Vpu adopts an experimentally confirmed kink within its TMD which was reported as early as 2002/3 prior to experimental findings [98,99]. Ser-24 has been marked as a putative candidate involved in the kink [98] and supported by extensive simulations of a Vpu monomer [100]. Computational analysis suggests a range of residues involved in the kink which are close to the residues marked by experiments, Ile-17 [42].

In the case of p7 of HCV, the idea of a titrable histidine within TMD1 of the protein facing a putative pore can still be validated with models of monomers derived from experiments which are assembled into a bundle. Protein p7 in a parallel aligned arrangement of the two membrane spanning segments is extensively simulated [87,88]. Analysis of the TMDs using RMSF data allows us to support the experimental findings [47] that both of the TMDs are literally separated into two 'sub-helical' segments with alternate dynamics. Other simulation studies rely on available experimentally derived structures of monomeric p7 to simulate bundle structures [92].

Structures of cytoplasmic parts of the VCPs have not been generated using purely computational methods. There is one report using sequence alignment of M2 with Vpu to propose structural features of M2 [101].

2.5. Predicting the oligomeric state

The protocols described to derive an oligomeric structure require the number of monomers to form the bundle. In the case of M2 the number of monomers forming the bundle is known experimentally using SDS-PAGE [69]. Protein 2B of polio/coxsackie virus is experimentally proposed to be a tetramer based on experiments with 2B attached to maltose-binding protein [102]. Protein 3a of SARS-CoV is found to form a tetramer out of two dimers [76] while E5 of HPV-16 is found to be a dimer [103] which forms hexamers [20]. The oligomeric state is identified in all cases by expressed and purified protein constructs using SDS-PAGE.

In other cases such as Vpu, this number of monomers is only estimated since experiments do not deliver unambiguous results. Based on pore size estimations relevant for ions to pass the Vpu bundle should exist of five monomers [71]. Thus the pentamer is used in computational modeling studies [71]. In a combined computational-experimental study, evidence for a pentameric state as the smallest unit is given [98]. Synthetic peptides (from SPPS) corresponding to extended segments of the TMD of Vpu have been reconstituted into artificial lipid bilayers to identify channel activity [98]. The observed conductance levels have been correlated with conductance estimates calculated from minimum pore sizes obtained from a sequence of four up to six computational derived bundle models of the respective segments using the program HOLE [104]. Based on these investigations the tetrameric bundle has been excluded as an ion conducting structure.

Simulations of pentameric and hexameric short Vpu peptides including the TMD in an octane slab embedded in water applying the CHARMM19 ff suggest that the pentameric bundle should be the most stable one [105]. The criteria are that in the hexameric bundle one of the TMDs escapes the circular arrangement of the TMDs. A similar situation is also reported for pentameric arrangements of TMDs of Vpu in explicit lipid/water system using the Gromos f96 (ffG45a3) ff [96].

In another study, the number of monomers forming a functional bundle is estimated to be five on symmetry considerations and energy estimates using classical and replica exchange MD simulations of tetra- to hexameric bundle architectures [91]. Dimer and trimer have not assembled in REMD simulations while the tetra- to hexamer bundles did so. Consequent repeated classical MD with the tetra- to hexamers using CHARMM22 ff. reveals an intact cyclic pentamer after a 10 ns MD simulation while the other two bundles collapse.

At this stage the question of how many monomers finally form the bundle is mainly addressed to Vpu since for most of the other VCPs the oligomeric state is identified experimentally. The major assumption is that the protein should follow the barrel-stave model since in the case of Vpu, distinct conductance states are experimentally observed. A toroidal model has so far not yet been considered in simulation studies as well as in none of the VCP-bundle models. It seems that energetic reasons for either one of the models are not explored to date. It's mainly visual inspection of the bundle architecture and whether it remains in a circular shape which is taken as the main criteria of whether or not the bundle represents a reliable model. Generally, computing used to predicting the oligomeric state is a challenge to be met.

2.6. Sequence alignment to derive functional information

The VCPs are assumed to fulfill a similar role as the host companions albeit putatively in a less precise and selective manner. It is tempting to speculate that the sequences have some ancestral relation to the host proteins as proposed for e.g. Vpu [106]. From a sequence relation there would eventually also be a functional and structural relation. In an attempt to address this question sequence alignment studies have been done for Vpu with ion channels and a toxin [107]. Alignment of the TMD of Vpu especially with pore lining TMDs of M2 from nAChR, and TMD αA from toxin ClyA is identified. In other cases the Vpu TMD sequence also matches with those of other ion channels which are not lining the pore. This study underlines the putative channel–pore dualism claimed experimentally for Vpu [16].

Screening of other polytopic VCPs such as p7 of HCV, 2B of polio virus and 3a of SARS-CoV reveals that the proteins with two TMDs, p7 and 2B from both polio and coxsackie viruses, align with pore lining TMDs of the MscL while 3a with its three TMDs matches best with those TMDs of ligand gated ion channels [108]. It is now tempting to speculate that as more TMDs are available as more the viral proteins become 'host-like'. With this, one can ask whether the VCPs with two TMDs in this case should sense eventual stress caused by curvature within the membrane. Likewise, are VCPs with more TMDs needed to conduct more precise tasks?

There is strong sequence alignment of 2B of coxsackie virus with M4 and M6 of the TM sector of human RyR2 [109]. Both RyR2 segments are not pore lining suggesting that 2B can also be falsely inserted during the RyR2 assembly process leading to miss-functioning RyR2 receptors. Thus, 2B could also have a non-ion channel related task in the viral infectivity cycle.

Looking over the fence, from the alignment study it is suggested that the bitopic VCPs could have some pore like activity with low selectivity and permeability for small molecules while increasing complexity expressed in an increase of the number of TMDs per monomer allows for more 'gated' behavior of the assembled proteins. In terms of a multi-tasking protein, smaller VCPs could act as building block replacements (or attachment) to harm host channels (and other membrane proteins of the host).

2.7. Ion selectivity

Assumption of a pentameric assembly of the TMD of Vpu ion selectivity of the protein bundles has been addressed using equilibrated bundle models from a 10 ps restrained MD simulation [71]. Potential energy profiles of ion/channel interaction of Na- and Cl-ions along the pore axis have been generated. Interaction profiles at the C terminal side of the pore have been favorable for Na-ions due to the ring of serines surrounding the pore at that side. Generally, this result matches experimental findings which report Vpu of HIV-1 to be weak (5–6 fold) cation specific [8]. However in a recent experimental study using bilayer recordings the data are interpreted in terms of a simultaneous cation/anion flux [16].

PMF calculations have been conducted on a series of monovalent ions to assess the selectivity of a pentameric bundle of Vpu [110]. The wave-like pattern of the PMF values along the pore axis supports the idea that the serines can attract the ions but then the hydrophobic tail towards the N terminal side imposes an energy barrier to any of the ions. The PMF values have been calculated from simulations (i) varying the stiffness of the spring for pulling the ion through the pore to derive initial configuration snapshots for the PMF calculations and (ii) the width of the bundle structure. Independent of these conditions, cations seems to adopt the lower PMF amplitude and are preferred within in the bundle. The differences between anions and cations are not quantified and seen to be marginal. Thus, the data support the experimental findings of the in both cases weak ion selectivity and simultaneous cation/ion permeation.

PMF calculations have also been used to predict selectivity of one of the shortest VCPs found to date, 8a of SARS-CoV [111] (Fig. 3, left). Calculations on all physiological relevant ions, Na-, K-, Cl- and Ca-ions, reveal a slight preference for cations which is confirmed by conductance experiments [112].

Another model for which selectivity is addressed by means of computation is p7 [113]. In a model, in which the TMDs of the monomer are aligned parallel and assembled into a hexameric bundle there is a constant voltage applied across the simulation box (Fig. 3, right). In a configuration in which relevant pore lining histidines have been uncharged the simulations reveal that e.g. both Cl- and K- or Ca-ions simultaneously permeate across the pore with a preference in numbers for the Cl-ions.

For M2 influenza A ion selectivity studies are limited since very early in the field of M2 research it became apparent that M2 conducts protons. Since protons or H_3O^+ is not parameterized in any of the ffs, respective simulations have not been conducted as mentioned above. Important in the investigations of M2 is the criteria of whether the bundle structure allows for the existence of a continuous water column during the simulation [84,93].

2.8. Gating

Mechanical features of M2 of influenza A are usually derived from classical MD simulation of the prepositioned bundles. In the case of M2 complex dynamics have been proposed [84,93]. Simulations have also included the pH dependent mechanics of the M2 bundle by protonating each of the relevant His-17 residues individually and separately in the bundle [114,115]. Detailed mechanical features of the dynamics of the histidines when in a neutral state are revealed [116]. Another classical MD simulation gives the suggestion that a second gate within the pore of M2 is formed by the four Val-27s which are able to disrupt the water column within the pore [117].

Using second generation MS-EVB2 models on conformations of the M2 channel derived from classical MD simulations a detailed picture of the mechanism of function has been developed [118]. It is suggested from these simulations that the channel allows the proton to pass the ring of four histidines (His-17) rather than a hydronium ion. Similar advanced simulation studies on the gating of other VCPs are lacking.

2.9. Structural plasticity suggested by computer simulations

Two of the VCPs are challenging the field;these are Vpu of HIV-1 and p7 of HCV. For both proteins the numbers of monomers forming a functional pore are not defined experimentally (for extensive experimental studies see [95]). Vpu is supposed not to exceed the pentameric or hexameric state [95,98]. Protein p7 is experimentally found in hexameric and heptameric states. At this state, classical MD simulations try to support any of these numbers by studying preorganized monomers being docked into oligomers [92,96,98]. As an analytical tool structural features such as tilt angles, number of hydrogen-bonds formed between monomers or water dynamics within the pore are used. In both cases, Vpu and p7, it is speculated that the proteins can exist in alternate oligomeric states either during the generation of the final bundles or at equilibrium. Handedness may be irrelevant for functioning (e.g. Vpu [96]). Protein p7 bundle structure is flexible and can adapt to changes in lipid composition reflected in e.g. altered lipid thickness [92]. Internal protein dynamics in this protein also seem to be pulsatile and highly dynamic [88]. As an interesting feature of the MD simulations, larger bundles allow for water filled pores during the simulation which is used as a highly plausible argument for the 'correctness' of the bundle structure [92]. Thus, a gating mechanism triggered by a change of the oligomeric state rather than protein internal conformational changes could be discussed. Also, for M2 analysis of early simulation data covering 2 ns have been interpreted in breathing motions of the tetramer [94].

2.10. Coarse graining

Coarse-graining may be a solution to the pressing questions of predicting e.g. oligomerization of VCPs. In this respect, CGMD simulations can be applied with models obtained from either computational modeling or experimental data and used in large scale lipid membranes. Since coarse graining of the structure will lead to a freezing of the dynamics of the proteins, the results can be seen on the basis of the parameters used to describe non-bonded interactions. Thus steric and diffusive features will be a relevant output of the simulations.

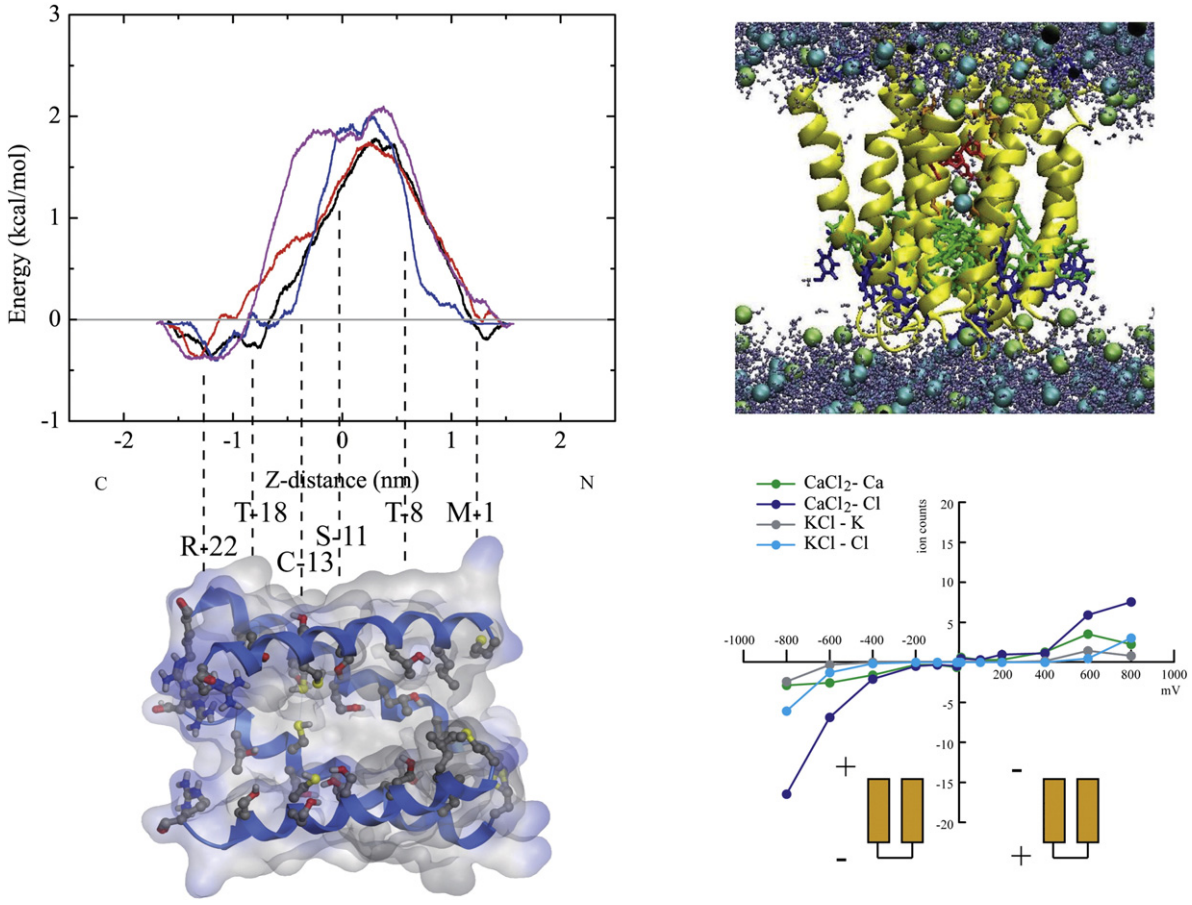

Fig. 3. Computational model of pentameric 8a bundle built from the first 22 amino acids and the potential of mean force (PMF) profile for a Na- (black), K- (red), Cl- (pink) and Ca-ion (blue) (left side) (see also figure 4 in [111]). One of the TMD of 8a is removed to see inside the lumen of the pore. A structural representation of a hexameric p7 bundle (HCV) simulated in the presence of a 1 M solution of $CaCl_2$ at the end of a 200 ns MD simulation (right side) (see also figures 3A and 4 in [113]). The bundle is embedded into a hydrated (water shown as lichorice triangles) lipid bilayer (lipid molecules are omitted for clarity). Ca-ions are shown in green, Cl-ions in cyan. Ion permeation when applied a set of voltages across the membrane system is shown in an I/V type diagram where the y-axis shows the ion counts.

Another coarse grained technique is the BFM. It is used to deliver generic information which is based on the principle of size exclusion. Originally, the method was intended to propose the organization and assembly of polymers [119]. The beads used are not parameterized. The fold of rhodopsin has been modeled [120] as well as the mechanism of oligomerization of prion proteins [121] and as well as the fold of rhodopsin. In recent reports the penetration of amphiphilic copolymers into lipid membranes has been investigated on the basis of the BFM [122,123]. The beads representing the molecules as well as the beads representing water both have been parameterized according to macroscopic properties such as degree of hydrophobicity to foster relevant interactions. It is up to future investigations to find out how much BFM contributes to the pressing question of fold of the extramembrane parts of the VCPs and the degree of oligomerization.

2.11. Drugs

Large drug screening reports using docking approaches are sparse for VCPs. Due to the unprecedented situation of available crystal structures with drugs bound to M2 of influenza A classical MD simulations are performed to explore the stability of the protein–ligand model [124]. Relative free energies of drug derivatives are obtained via TCP method with the M2 structure to which the drug amantadine is bound [125]. PMF calculations have been used to explore the energetics of the drugs found in experiments in contact with M2 of influenza A [126,127] and B [127].

Interactions of drugs with the VCPs have mostly been modeled for p7 using available docking software with computationally derived models [87,128]. In other studies, experimentally based structures have been used [51].

2.12. Information output from computational modeling

Definition of structure is based on the quality of the secondary structure prediction programs and limited to the prediction of the length of the TMDs. These prediction programs serve well to deliver a putative starting structure which could be further refined by MD simulations. However, with the bundle model of p7 derived from NMR experiments [52], the bar has been raised. Such a structure could not have been proposed with the current techniques and protocols. It remains up to future studies to deliver solutions for the generation of plausible monomeric and oligomeric structures on the basis of the primary and secondary structures.

Modeling the oligomeric state of the VCPs is still in the need of knowing the numbers of monomers forming the oligomeric state and with it the bundle structure still depends on experimental data. Structural information then depends on the applied techniques such as docking approaches and classical MD simulations. Approaching the oligomeric state by allowing a diffusional degree of freedom using CG models has not yet been reported.

Computational modeling data support the experimentally emerging picture of dynamic and GT specific models of individual VCPs. This stand in contrast to the knowledge about the ion channels of the host which

are larger and found in defined oligomeric states and with a well-defined structure and gating behavior. The cytoplasmic parts of many of the VCPs are still a white spot in computer based structure modeling of the VCPs.

3. Outlook to unresolved questions

The simulation techniques rely upon structural models or if fully used as a self-contained approach on simplified assumptions. The dynamics within the proteins can then be readily investigated and specific features can be proposed. In the field of VCPs there is a hypothesis emerging that is 'defined channel versus crude assemblies'. The proteins may be seen as highly dynamic in their quaternary structure and are already captured by experiments being in a kind of oligomerization equilibrium within the lipid membrane. Computational studies using coarse grained techniques could spear head and explore the hypothesis.

Another feature for which the VCP could serve as an interesting playground is the mechanism of how a pore is finally formed which in the end allows for ion/substrate permeation. Are defined channel formed or rather crude assemblies in which eventually pores are formed? These assemblies would also able to interact with host or viral factors. In contrast to ion channels of the host, where structural information is emerging thoroughly by now, structural data for viral channels are sparse. This is due to experimental difficulties of handling small peptides and the small proteins in general with available preparation techniques.

Transparency document

The Transparency document associated with this article can be found, in online version.

Acknowledgment

WBF thanks the National Science Council (NSC-101-2112-M-010-002-MY3), Taiwan, for financial support. MMK acknowledges a student-fellowship of National Yang-Ming University.

References

[1] L. Carrasco, The inhibition of cell functions after viral infection, FEBS Lett. 76 (1977) 11–15.
[2] L. Carrasco, Membrane leakiness after viral infection and a new approach to the development of antiviral agents, Nature 272 (1978) 694–699.
[3] J. Lama, L. Carrasco, Expression of poliovirus nonstructural proteins in *Escherichia coli* cells. Modificaion of membrane permeability induced by 2B and 3A, J. Biolumin. Chemilumin. 267 (1992) 15932–15937.
[4] M.A. Sanz, L. Perez, L. Carrasco, Semliki Forest virus 6K protein modifies membrane permeability after inducible expression in *Escherichia coli* cells, J. Biolumin. Chemilumin. 269 (1994) 12106–12110.
[5] K.C. Duff, R.H. Ashley, The transmembrane domain of influenza A M2 protein forms amantadine-sensitive proton channels in planar lipid bilayers, Virology 190 (1992) 485–489.
[6] C. Wang, K. Takeuchi, L.H. Pinto, R.A. Lamb, Ion channel activity of influenza A virus M_2 protein: characterization of the amantadine block, J. Virol. 67 (1993) 5585–5594.
[7] U. Schubert, A.V. Ferrer-Montiel, M. Oblatt-Montal, P. Henklein, K. Strebel, M. Montal, Identification of an ion channel activity of the Vpu transmembrane domain and its involvement in the regulation of virus release from HIV-1-infected cells, FEBS Lett. 398 (1996) 12–18.
[8] G.D. Ewart, T. Sutherland, P.W. Gage, G.B. Cox, The Vpu protein of human immunodeficiency virus type 1 forms cation-selective ion channels, J. Virol. 70 (1996) 7108–7115.
[9] W.B. Fischer, M.S.P. Sansom, Viral ion channels: structure and function, Biochim. Biophys. Acta 1561 (2002) 27–45.
[10] M.E. Gonzales, L. Carrasco, Viroporins, FEBS Lett. 552 (2003) 28–34.
[11] K. Wang, S. Xie, B. Sun, Viral proteins function as ion channels, Biochim. Biophys. Acta 1808 (2010) 510–515.
[12] W.B. Fischer, Y.-T. Wang, C. Schindler, C.-P. Chen, Mechanism of function of viral channel proteins and implications for drug development, Int. Rev. Cell Mol. Biol. 294 (2012) 259–321.
[13] J.L. Nieva, V. Madan, L. Carrasco, Viroporins: structure and biological functions, Nat. Rev. Microbiol. 10 (2012) 563–574.
[14] B. OuYang, J.J. Chou, The minimalist architectures of viroporins and their therapeutic implications, Biochim. Biophys. Acta 1838 (2014) 1058–1067.
[15] C. Scott, S. Griffin, Viroporins: structure, function and potential as antiviral targets, J. Gen. Virol. 96 (2015) 2000–2027.
[16] T. Mehnert, A. Routh, P.J. Judge, Y.H. Lam, D. Fischer, A. Watts, W.B. Fischer, Biophysical characterisation of Vpu from HIV-1 suggests a channel–pore dualism, Proteins 70 (2008) 1488–1497.
[17] K.J. Cho, B. Schepens, J.H. Seok, S. Kim, K. Roose, J.-H. Lee, R. Gallardo, E. Van Hamme, J. Schymkowitz, F. Rousseau, M. Müller, G. Howell, M. Harris, C. Fishwick, N. Stonehouse, R. Foster, G.E. Blair, S. Griffin, A. Macdonald, High-risk human papillomavirus E5 oncoprotein displays channel-forming activity sensitive to small-molecule inhibitors, J. Virol. 86 (2012) 5341–5351.
[18] K. Strebel, HIV-1 Vpu — an ion channel in search for a job, Biochim. Biophys. Acta 1838 (2014) 1074–1081.
[19] W.B. Fischer, L.-H. Li, D.R. Mahato, Y.-T. Wang, C. Chen, Viral channel proteins in intracellular protein–protein communication: Vpu of HIV-1, E5 of HPV16 and p7 of HCV, Biochim. Biophys. Acta 1838 (2014) 1113–1121.
[20] L.F. Wetherill, K.K. Holmes, M. Verow, M. Müller, G. Howell, M. Harris, C. Fishwick, N. Stonehouse, R. Foster, G.E. Blair, S. Griffin, A. Macdonald, High-risk human papillomavirus E5 oncoprotein displays channel-forming activity sensitive to small-molecule inhibitors, J. Virol. 86 (2012) 5341–5351.
[21] M. Montal, Vpu matchmakers as a therapeutic strategy for HIV infection, PLoS Pathog. 5 (2009), e1000246.
[22] K.C. Duff, S.M. Kelly, N.C. Price, J.P. Bradshaw, The secondary structure of influenza A M2 transmembrane domain. A circular dichroism study, FEBS Lett. 311 (1992) 256–258.
[23] F.A. Kovacs, T.A. Cross, Transmembrane four-helix bundle of influenza A M2 protein channel: structural implications from helix tilt and orientation, Biophys. J. 73 (1997) 2511–2517.
[24] A. Kukol, P.D. Adams, L.M. Rice, A.T. Brunger, I.T. Arkin, Experimentally based orientational refinement of membrane protein models: a structure for the influenza A M2 H^+ channel, J. Mol. Biol. 286 (1999) 951–962.
[25] K. Nishimura, S. Kim, L. Zhang, T.A. Cross, The closed state of a H^+ channel helical bundle combining precise orientational and distance restraints from solid state NMR, Biochemistry 41 (2002) 13170–13177.
[26] C. Tian, K. Tobler, R.A. Lamb, L.H. Pinto, T.A. Cross, Expression and initial structural insights from solid-state NMR of the M2 proton channel from influenza A virus, Biochemistry 41 (2002) 11294–11300.
[27] C. Tian, P.F. Gao, L.H. Pinto, R.A. Lamb, T.A. Cross, Initial structural and dynamic characterization of the M2 protein transmembrane and amphipathic helices in lipid bilayers, Protein Sci. 12 (2003) 2597–2605.
[28] J.R. Schnell, J.J. Chou, Structure and mechanism of the M2 proton channel of influenza A virus, Nature 451 (2008) 591–595.
[29] A.L. Stouffer, R. Acharya, D. Salom, A.S. Levine, L. Di Constanzo, C.S. Soto, V. Tereshko, V. Nanda, S. Stayrook, W.F. DeGrado, Structural basis for the function and inhibition of an influenza virus proton channel, Nature 451 (2008) 596–599.
[30] S.D. Cady, K. Schmidt-Rohr, J. Wang, C.S. Soto, W.F. DeGrado, M. Hong, Structure of the amantadine binding site of influenza M2 proton channels in lipid bilayers, Nature 463 (2010) 689–692.
[31] R.M. Pielak, K. Oxenoid, J.J. Chou, Structural investigation of rimantadine inhibition of the AM2–BM2 chimera channel of influenza viruses, Structure 19 (2011) 1655–1663.
[32] J. Wang, Y. Wu, C. Ma, G. Fiorin, J. Wang, L.H. Pinto, R.A. Lamb, M.L. Klein, W.F. DeGrado, Structure and inhibition of the drug-resistant S31N mutant of the M2 ion channel of influenza A virus, Proc. Natl. Acad. Sci. U. S. A. 110 (2013) 1315–1320.
[33] Y. Wu, B. Canturk, H. Jo, C. Ma, E. Gianti, G. Florin, L.H. Pinto, R.A. Lamb, M.L. Klein, J. Wang, W.F. DeGrado, Flipping in the pore: discovery of dual inhibitors that bind in different orientations to the wild-type versus the amantadine-resistant S31N mutant of the influenza A virus M2 proton channel, J. Am. Chem. Soc. 136 (2014) 17987–17995.
[34] D. Willbold, S. Hoffmann, P. Rösch, Secondary structure and tertiary fold of the human immunodeficiency virus protein U (Vpu) cytoplasmatic domain in solution, Eur. J. Biochem. 245 (1997) 581–588.
[35] V. Wray, T. Federau, P. Henklein, S. Klabunde, O. Kunert, D. Schomburg, U. Schubert, Solution structure of the hydrophilic region of HIV-1 encoded virus protein U (Vpu) by CD and ^{1}H NMR-spectroscopy, Int. J. Pept. Protein Res. 45 (1995) 35–43.
[36] T. Federau, U. Schubert, J. Floßdorf, P. Henklein, D. Schomburg, V. Wray, Solution structure of the cytoplasmic domain of the human immunodeficiency virus type 1 encoded virus protein U (Vpu), Int. J. Pept. Protein Res. 47 (1996) 297–310.
[37] M. Wittlich, B.W. Koenig, M. Stoldt, H. Schmidt, D. Willbold, NMR structural characterization of HIV-1 virus protein U cytoplasmic domain in the presence of dodecylphosphatidylcholine micelles, FEBS J. 276 (2009) 6560–6575.
[38] M. Wittlich, B.W. Koenig, D. Willbold, Structural consequences of phosphorylation of two serine residues in the cytiplasmic domain of HIV-1 VpU, J. Pept. Sci. 14 (2008) 804–810.
[39] G. Coadou, N. Evrard-Todeschi, J. Gharbi-Benarous, R. Benarous, J.-P. Girault, Conformational analysis by NMR and molecular modelling of the 41–62 hydrophilic region of HIV-1 encoded virus protein U (Vpu). Effect of the phosphorylation on sites 52 and 56, C.R. Acad. Sci., Ser. IIc: Chim. 4 (2001) 751–758.
[40] F.M. Marassi, C. Ma, H. Gratkowski, S.K. Straus, K. Strebel, M. Oblatt-Montal, M. Montal, S.J. Opella, Correlation of the structural and functional domains in the membrane protein Vpu from HIV-1, Proc. Natl. Acad. Sci. U. S. A. 96 (1999) 14336–14341.
[41] V. Wray, R. Kinder, T. Federau, P. Henklein, B. Bechinger, U. Schubert, Solution structure and orientation of the transmembrane anchor domain of the HIV-1-encoded virus protein U by high resolution and solid-state NMR spectroscopy, Biochemistry 38 (1999) 5272–5282.

[42] S.H. Park, A.A. Mrse, A.A. Nevzorov, M.F. Mesleh, M. Oblatt-Montal, M. Montal, S.J. Opella, Three-dimensional structure of the channel-forming trans-membrane domain of virus protein "u" (Vpu) from HIV-1, J. Mol. Biol. 333 (2003) 409–424.

[43] P. Henklein, R. Kinder, U. Schubert, B. Bechinger, Membrane interactions and alignment of structures within the HIV-1 Vpu cytoplasmic domain: effect of phosphorylation of serines 52 and 56, FEBS Lett. 482 (2000) 220–224.

[44] C. Ma, F.M. Marassi, D.H. Jones, S.K. Straus, S. Bour, K. Strebel, U. Schubert, M. Oblatt-Montal, M. Montal, S.J. Opella, Expression, purification, and activities of full-length and truncated versions of the integral membrane protein Vpu from HIV-1, Protein Sci. 11 (2002) 546–557.

[45] H. Zhang, E.C. Lin, B.B. Das, Y. Tian, S.J. Opella, Structural determination of virus protein U from HIV-1 by NMR in membrane environments, Biochim. Biophys. Acta 1848 (2015) 3007–3018.

[46] M. Skasko, Y. Wang, Y. Tian, A. Tokarev, J. Munguia, A. Ruiz, E.B. Stephens, S.J. Opella, J. Guatelli, HIV-1 Vpu protein antagonizes the innate restriction factor BST-2 via lipid-embedded helix–helix interactions, J. Biolumin. Chemilumin. 287 (2012) 58–67.

[47] G.A. Cook, S.J. Opella, NMR studies of the p7 protein from hepatitis C virus, Eur. Biophys. J. 39 (2010) 1097–1104.

[48] G.A. Cook, S.J. Opella, Secondary structure, dynamics, and architecture of the p7 membrane protein from hepatitis C virus by NMR spectroscopy, Biochim. Biophys. Acta 1808 (2011) 1448–1453.

[49] R. Montserret, N. Saint, C. Vanbelle, A.G. Salvay, J.P. Simorre, C. Ebel, N. Sapay, J.-G. Renisio, A. Böckmann, E. Steinmann, T. Pietschmann, J. Dubuisson, C. Chipot, F. Penin, NMR structure and ion channel activity of the p7 protein from hepatitis C virus, J. Biolumin. Chemilumin. 285 (2010) 31446–31461.

[50] G.A. Cook, L.A. Dawson, Y. Tian, S.J. Opella, Three-dimensional structure and interaction studies of hepatitis C virus p7 in 1,2-dihexanoyl-sn-glycero-3-phosphatidylcholine by solution nuclear magnetic resonance, Biochemistry 52 (2013) 5295–5303.

[51] T.L. Foster, G.S. Thompson, A.P. Kalverda, J. Kankanala, M. Bentham, L.F. Wetherill, J. Thompson, A.M. Barker, D. Clarke, M. Noerenberg, A.R. Pearson, D.J. Rowlands, S.W. Homans, M. Harris, R. Foster, S. Griffin, Structure-guided design affirms inhibitors of hepatitis C virus p7 as a viable class of antivirals targeting virion release, Hepatology 59 (2014) 408–422.

[52] B. OuYang, S. Xie, M.J. Berardi, X. Zhao, J. Dev, W. Yu, B. Sun, J.J. Chou, Unusual architecture of the p7 channel from hepatitis C virus, Nature 498 (2013) 521–525.

[53] S.D.C. Griffin, L.P. Beales, D.S. Clarke, O. Worsfold, S.D. Evans, J. Jäger, M.P.G. Harris, D.J. Rowlands, The p7 protein of hepatitis C virus forms an ion channel that is blocked by the antiviral drug, amantadine, FEBS Lett. 535 (2003) 34–38.

[54] D. Clarke, S. Griffin, L. Beales, C.S. Gelais, S. Burgess, M. Harris, D. Rowlands, Evidence for the formation of a heptameric ion channel complex by the hepatitis C virus p7 protein in vitro, J. Biolumin. Chemilumin. 281 (2006) 37057–37068.

[55] P. Luik, C. Chew, J. Aittoniemi, J. Chang, P. Wentworth Jr., R. Dwek, P.C. Biggin, C. Vénien-Bryan, N. Zitzmann, The 3-dimensional structure of the hepatitis C virus p7 ion channel by electron microscopy, Proc. Natl. Acad. Sci. U. S. A. 106 (2009) 12712–12716.

[56] C.G. Ullman, P.I. Haris, B. Kell, J. Cason, R.J. Jewers, J.M. Best, V.C. Emery, S.J. Perkins, Hypothetical structure of the membrane-associated E5 oncoprotein of human papillomavirus type 16, Biochem. Soc. Trans. 22 (1994) 439S.

[57] A. Alonso, J. Reed, Modelling of the human papillomavirus type 16 E5 protein, Biochim. Biophys. Acta 1601 (2002) 9–18.

[58] A.V. Guzzo, The influence of amino-acid sequence on protein structure, Biophys. J. 5 (1965) 809–822.

[59] W.B. Fischer, H.-J. Hsu, From sequence to structure to mechanism — viral channel proteins, in: G. Fung (Ed.) Sequence and Genome Analysis: Methods and Application II, vol. 2, iConcept Press, Hong Kong, 2013.

[60] R.A. Lamb, S.L. Zebedee, C.D. Richardson, Influenza virus M_2 protein is an integral membrane protein expressed on the infected-cell surface, Cell 40 (1985) 627–633.

[61] K. Strebel, T. Klimkait, M.A. Martin, Novel gene of HIV-1, *vpu*, and its 16-kilodalton product, Science 241 (1988) 1221–1223.

[62] J. Kyte, R.F. Doolittle, A simple method for displaying the hydropathic character of a protein, J. Mol. Biol. 157 (1982) 105–132.

[63] V.J. Bubb, D.J. McCance, R. Schlegel, DNA sequence of the HPV-16 E5 ORF and the structural conservation of its encoded protein, Virology 163 (1988) 243–246.

[64] C. Lin, B.D. Lindenbach, B.M. Pragai, D.W. McCourt, C.M. Rice, Processing in the hepatitis C virus E2-NS2 region: identification of p7 and two distinct E2-specific products with different C termini, J. Virol. 68 (1994) 5063–5073.

[65] K. Elbers, N. Tautz, P. Becher, D. Stoll, T. Rumenapf, H.J. Thiel, Processing in the pestivirus E2-NS2 region: identification of proteins p7 and E2p7, J. Virol. 70 (1996) 4131–4135.

[66] T.P. Hopp, K.R. Woods, Prediction of protein antigenic determinants from amino acid sequences, Proc. Natl. Acad. Sci. U. S. A. 78 (1981) 3824–3828.

[67] F.J.M. van Kuppeveld, J.M.D. Galama, J. Zoll, P.J.J.C. van den Hurk, W.J.G. Melchers, Coxsackie B3 virus protein 2B contains a cationic amphipathic helix that is required for viral RNA replication, J. Virol. 70 (1996) 3876–3886.

[68] D. Eisenberg, E. Schwarz, M. Komaromy, R. Wall, Analysis of membrane and surface protein sequences with the hydrophobic moment plot, J. Mol. Biol. 179 (1984) 125–142.

[69] R.J. Sugrue, A.J. Hay, Structural characteristics of the M2 protein of influenza A viruses: evidence that it forms a tetrameric channel, Virology 180 (1991) 617–624.

[70] M.S.P. Sansom, I.D. Kerr, Influenza virus M_2 protein: a molecular modelling study on the ion channel, Protein Eng. 6 (1993) 65–74.

[71] A.L. Grice, I.D. Kerr, M.S.P. Sansom, Ion channels formed by HIV-1 Vpu: a modelling and simulation study, FEBS Lett. 405 (1997) 299–304.

[72] U. Schubert, P. Henklein, B. Boldyreff, E. Wingender, K. Strebel, T. Porstmann, The human immunodeficiency virus type 1 encoded Vpu protein is phosphorylated by casein kinase-2 (CK-2) at positions Ser52 and Ser54 within a predicted a-helix-turn-a-helix-motif, J. Mol. Biol. 236 (1994) 16–25.

[73] G. Patargias, N. Zitzmann, R. Dwek, W.B. Fischer, Protein–protein interactions: modeling the hepatitis C virus ion channel p7, J. Med. Chem. 49 (2006) 648–655.

[74] F.J.M. van Kuppeveld, W.J.G. Melchers, K. Kirkegaard, J.R. Doedens, Structure–function analysis of coxsackie B3 virus protein 2B, Virology 227 (1997) 111–118.

[75] G. Patargias, T. Barke, A. Watts, W.B. Fischer, Model generation of viral channel forming 2B protein bundles from polio and coxsackie viruses, Mol. Membr. Biol. 26 (2009) 309–320.

[76] W. Lu, B.-J. Zheng, K. Xu, W. Schwarz, L. Du, C.K.L. Wong, J. Chen, S. Duan, V. Deubel, B. Sun, Severe acute respiratory syndrome-associated coronavirus 3a protein forms an ion channel and modulates virus release, Proc. Natl. Acad. Sci. U. S. A. 103 (2006) 12540–12545.

[77] H.-J. Hsu, W.B. Fischer, In silico investigations of possible routes of assembly of ORF 3a from SARS-CoV, J. Mol. Model. 18 (2011) 501–514.

[78] G. Baumann, P. Mueller, A molecular model of membrane excitability, J. Supramol. Struct. 2 (1974).

[79] H.W. Huang, Action of antimicrobial peptides: two-state model, Biochemistry 39 (2000) 8347–8352.

[80] M.T. Tosteson, L.H. Pinto, L.J. Holsinger, R.A. Lamb, Reconstitution of the influenza virus M_2 ion channel in lipid bilayers, J. Membr. Biol. 142 (1994) 117–126.

[81] L.R. Forrest, W.F. DeGrado, G.R. Dieckmann, M.S.P. Sansom, Two models of the influenza A M2 channel domain: verification by comparison, Fold. Des. 3 (1998) 443–448.

[82] I.D. Kerr, R. Sankararamakrishnan, O.S. Smart, M.S.P. Sansom, Parallel helix bundles and ion channels: molecular modelling via simulated annealing and restrained molecular dynamics, Biophys. J. 67 (1994) 1501–1515.

[83] F. Cordes, A. Kukol, L.R. Forrest, I.T. Arkin, M.S.P. Sansom, W.B. Fischer, The structure of the HIV-1 Vpu ion channel: modelling and simulation studies, Biochim. Biophys. Acta 1512 (2001) 291–298.

[84] M.S.P. Sansom, I.D. Kerr, S.G. R., H.S. Son, The influenza A virus M2 channel: a molecular modelling and simulation study, Virology 233 (1997) 163–173.

[85] W.B. Fischer, M. Pitkeathly, B.A. Wallace, L.R. Forrest, G.R. Smith, M.S. Sansom, Transmembrane peptide NB of influenza B: a simulation, structure, and conductance study, Biochemistry 39 (2000) 12708–12716.

[86] J. Krüger, W.B. Fischer, Assembly of viral membrane proteins, J. Chem. Theory Comput. 5 (2009) 2503–2513.

[87] Y.-T. Wang, H.-J. Hsu, W.B. Fischer, Computational Modeling of the p7 Monomer From HCV and Its Interaction With Small Molecule Drugs, 2SpringerPlus, 2013 324.

[88] M.M. Kalita, S. Griffin, J.J. Chou, W.B. Fischer, Genotype-specific differences in structural features of hepatitis C virus (HCV) p7 membrane protein, Biochim. Biophys. Acta 1848 (2015) 1383–1392.

[89] A. Kukol, I.T. Arkin, Vpu transmembrane peptide structure obtained by site-specific fourier transform infrared dichroism and global molecular dynamics searching, Biophys. J. 77 (1999) 1594–1601.

[90] P.B. Moore, Q. Zhong, T. Husslein, M.L. Klein, Simulation of the HIV-1 Vpu transmembrane domain as a pentameric bundle, FEBS Lett. 431 (1998) 143–148.

[91] S. Padhi, N. Khan, S. Jameel, U.D. Priyakumar, Molecular dynamic simulations reveal the HIV-1 Vpu transmembrane protein to form stable pentamers, PLoS One 8 (2013), e79779.

[92] D.E. Chandler, F. Penin, K. Schulten, C. Chipot, The p7 protein of hepatitis C virus forms structurally plastic, minimalist ion channels, PLoS Comput. Biol. 8 (2012), e1002702.

[93] Q. Zhong, T. Husslein, P.B. Moore, D.M. Newns, P. Pattnaik, M.L. Klein, The M2 channel of influenza A virus: a molecular dynamics study, FEBS Lett. 434 (1998) 265–271.

[94] L.R. Forrest, A. Kukol, I.T. Arkin, D.P. Tieleman, M.S. Sansom, Exploring models of the influenza A M2 channel: MD simulations in a phospholipid bilayer, Biophys. J. 78 (2000) 55–69.

[95] J.-X. Lu, S. Sharpe, R. Ghirlando, W.-M. Yau, R. Tycko, Oligomerization state and supramolecular structure of the HIV-1 Vpu protein transmembrane segment in phospholipid bilayers, Protein Sci. 19 (2010) 1877–1896.

[96] L.-H. Li, H.-J. Hsu, W.B. Fischer, Assembling vrial channel forming proteins: Vrpu from HIV-1, Biopolymers 99 (2013) 517–529.

[97] L.-H. Li, H.-J. Hsu, W.B. Fischer, Qualitative computational bioanalytics: assembly of viral channel-forming peptides around mono and divalent ions, Biochem. Biophys. Res. Commun. 442 (2013) 85–91.

[98] F.S. Cordes, A.D. Tustian, M.S. Sansom, A. Watts, W.B. Fischer, Bundles consisting of extended transmembrane segments of Vpu from HIV-1: computer simulations and conductance measurements, Biochemistry 41 (2002) 7359–7365.

[99] I. Sramala, V. Lemaitre, J.D. Faraldo-Gomez, S. Vincent, A. Watts, W.B. Fischer, Molecular dynamics simulations on the first two helices of Vpu from HIV-1, Biophys. J. 84 (2003) 3276–3284.

[100] J. Krüger, W.B. Fischer, Exploring the conformational space of Vpu from HIV-1: a versatile adaptable protein, J. Comput. Chem. 29 (2008) 2416–2424.

[101] J.W. Saldanha, P.E. Czabotar, A.J. Hay, W.R. Taylor, A model for the cytoplasmic domain of the influenza A virus M2 channel by analogy to the HIV-1 Vpu protein, Protein Pept. Lett. 9 (2002) 495–502.

[102] A. Agirre, A. Barco, L. Carrasco, J.L. Nieva, Viroporin-mediated membrane permeabilization. Pore formation by nanostructural poliovirus 2B protein, J. Biolumin. Chemilumin. 277 (2002) 40434–40441.

[103] B. Kell, R.J. Jewers, J. Cason, F. Pakarian, J.N. Kaye, J.M. Best, Detection of E5 oncoprotein in human papillomavirus type 16-positive cervical scrapes using antibodies raised to synthetic peptides, J. Gen. Virol. 75 (1994) 2451–2456.
[104] O.S. Smart, J.G. Neduvelil, X. Wang, B.A. Wallace, M.S.P. Sansom, Hole: a program for the analysis of the pore dimensions of ion channel structural models, J. Mol. Graph. 14 (1996) 354–360.
[105] C.F. Lopez, M. Montal, J.K. Blasie, M.L. Klein, P.B. Moore, Molecular dynamics investigation of membrane-bound bundles of the channel-forming transmembrane domain of viral protein U from the human immunodeficiency virus HIV-1, Biophys. J. 83 (2002) 1259–1267.
[106] K. Hsu, J. Seharaseyon, P. Dong, S. Bour, E. Marbán, Mutual functional destruction of HIV-1 Vpu and host TASK-1 channel, Mol. Cell 14 (2004) 259–267.
[107] W.B. Fischer, H.J. Hsu, Viral channel forming proteins — modelling the target, Biochim. Biophys. Acta 1808 (2011) 561–571.
[108] C. Schindler, W.B. Fischer, Sequence alignment of viral channel proteins with cellular ion channels and toxins, J. Comp. Biol. 19 (2012) 1060–1072.
[109] R. Schilling, R.H.A. Fink, W.B. Fischer, MD simulations of the central pore of ryanodine receptors and sequence comparison with 2B protein from coxsackie virus, Biochim. Biophys. Acta 1838 (2014) 1122–1131.
[110] G. Patargias, H. Martay, W.B. Fischer, Reconstructing potentials of mean force from short steered molecular dynamics simulations of Vpu from HIV-1, J. Biomol. Struct. Dyn. 26 (2009) 1–12.
[111] H.-J. Hsu, M.-H. Lin, C. Schindler, W.B. Fischer, Structure based computational assessment of channel properties of assembled ORF-8a from SARS-CoV, Proteins 83 (2015) 300–308.
[112] C.-C. Chen, J. Krüger, I. Sramala, H.-J. Hsu, P. Henklein, Y.-M.A. Chen, W.B. Fischer, ORF 8a of severe acute respiratory syndrome coronavirus forms an ion channel: experiments and molecular dynamics simulations, Biochim. Biophys. Acta 1808 (2011) 572–579.
[113] Y.-T. Wang, R. Schilling, R.H.A. Fink, W.B. Fischer, Ion-dynamics in hepatitis C virus p7 helical transmembrane domains — a molecular dynamics simulation study, Biophys. Chem. 192 (2014) 33–40.
[114] K.J. Schweighofer, A. Pohorille, Computer simulation of ion channel gating: the M_2 channel of influenza A virus in a lipid bilayer, Biophys. J. 78 (2000) 150–163.
[115] R. Acharya, V. Carnevale, G. Fiorin, B.G. Levine, A.L. Polishchuk, V. Balannik, I. Samish, R.A. Lamb, L.H. Pinto, W.F. DeGrado, M.L. Klein, Structure and mechanism of proton transport through the transmembrane tetrameric M2 protein bundle of the influenza A virus, Proc. Natl. Acad. Sci. U. S. A. 107 (2010) 15075–15080.
[116] H. Dong, G. Fiorin, W.F. DeGrado, M.L. Klein, Exploring histidine conformations in the M2 channel lumen of the influenza A virus at neutral pH via molecular simulations, J. Phys. Chem. Lett. 4 (2013) 3067–3071.
[117] M. Yi, T.A. Cross, H.-X. Zhou, A secondary gate as a mechanism for inhibition of the M2 proton channel by amantadine, J. Phys. Chem. B 112 (2008) 7977–7979.
[118] A.M. Smondyrev, G.A. Voth, Molecular dynamics simulation of proton transport through the influenza A virus M2 channel, Biophys. J. 83 (2002) 1987–1996.
[119] I. Carmesin, K. Kremer, The bond fluctuation method: a new effective algorithm for the dynamics of polymers in all spatial dimensions, Macromolecules 21 (1988) 2819–2823.
[120] C.-M. Chen, C.-C. Chen, Computer simulations of membrane protein folding: structure and dynamics, Biophys. J. 84 (2003) 1902–1908.
[121] D.-M. Ou, C.-C. Chen, C.-M. Chen, Contact-induced structure transformation in transmembrane prion propagation, Biophys. J. 92 (2007) 2704–2710.
[122] M. Werner, J.-U. Sommer, V.A. Baulin, Homo-polymers with balanced hydrophobicity translocate through lipid bilayers and enhance local solvent permeability, Soft Matter 8 (2012) 11714–11722.
[123] M. Werner, J.-U. Sommer, Translocation and induced permeability of random amphiphilic copolymers interaction with lipid bilayer membranes, Macromolecules 16 (2015) 125–135.
[124] E. Khurana, R.H. DeVane, M.D. Peraro, M.L. Klein, Computational study of drug binding to the membrane-bound tetrameric M2 peptide bundle from influenza A virus, Biochim. Biophys. Acta 1808 (2011) 530–537.
[125] P. Gkeka, S. Eleftheratos, A. Kolocouris, Z. Cournia, Free energy calculations reveal the origin of binding preference for aminoadamantane blockers of influenza A/M2TM pore, J. Chem. Theory Comput. 9 (2013) 1272–1281.
[126] R.-X. Gu, L.A. Liu, D.-Q. Wei, J.-G. Du, L. Liu, H. Liu, Free energy calculations on the two drug binding sites in the M2 proton channel, J. Am. Chem. Soc. 133 (2011) 10817–10825.
[127] Y. Zhang, H. Shen, M. Zhang, G. Li, Exploring the proton conductance and drug resistance of BM2 channel through molecular dynamics simulations and free energy calculations at different pH conditions, J. Phys. Chem. B 117 (2013) 982–988.
[128] L. Bichmann, Y.-T. Wang, W.B. Fischer, Docking assay of small molecule antivirals to p7 of HCV, Comput. Biol. Chem. 53 (2014) 308–317.
[129] S.H. Park, A.A. De Angelis, A.A. Nevzorov, C.H. Wu, S.J. Opella, Three-dimensional structure of the transmembrane domain of Vpu from HIV-1 in aligned phospholipid bicelles, Biophys. J. 91 (2006) 3032–3042.
[130] S.H. Park, S.J. Opella, Conformational changes induced by a single amino acid substitution in the *trans*-membrane domain of Vpu: implications for HIV-1 susceptibility to channel blocking drugs, Protein Sci. 16 (2007) 2205–2215.
[131] R.M. Pielak, J.J. Chou, Solution NMR structure of the V27A drug resistant mutant of influenza A M2 channel, Biochem. Biophys. Res. Commun. 401 (2010) 58–63.
[132] R.M. Pielak, J.R. Schnell, J.J. Chou, Mechanism of drug inhibition and drug resistance of influenza A M2 channel, Proc. Natl. Acad. Sci. U. S. A. 106 (2009) 7379–7384.
[133] J. Wang, R.M. Pielak, M.A. McClintock, J.J. Chou, Solution structure and functional analysis of the influenza B proton channel, Nat. Struct. Biol. 16 (2009) 1267–1271.
[134] S.D. Cady, T.V. Mishana, M. Hong, Structure of amantadine-bound M2 transmembrane peptide of influenza A in lipid bilayers from magic-angle-spinning solid-state NMR: the role of Ser31 in amantadine binding, J. Mol. Biol. 385 (2009) 1127–1141.
[135] J. Hu, T. Asbury, S. Achuthan, R. Bertram, J.R. Quine, R. Fu, T.A. Cross, Backbone structure of the amantadine-blocked trans-membrane domain M2 protein channel from influenza A virus, Biophys. J. 92 (2007) 4335–4343.
[136] M. Sharma, M. Yi, H. Dong, H. Qin, E. Peterson, D.D. Busath, H.-X. Zhou, T.A. Cross, Insight into the mechanism of the influenza A proton channel from a structure in a lipid bilayer, Science 330 (2010) 509–512.
[137] J. Wang, S. Kim, F. Kovacs, T.A. Cross, Structure of the transmembrane region of the M2 protein H^+ channel, Protein Sci. 10 (2001) 2241–2250.
[138] J. Hu, R. Fu, T.A. Cross, The chemical and dynamical influence of the anti-viral drug amantadine on teh M2 proton channel transmembrane domain, Biophys. J. 93 (2007) 276–283.
[139] H. Shen, J.J. Chou, MemBrain: improving the accuracy of predicting transmembrane helices, PLoS One 3 (2008), e2399.
[140] K. Hofmann, W. Stoffel, TMbase — a database of membrane spanning protein segments, Biol. Chem. Hoppe Seyler 374 (1993) 166.
[141] M. Cserzö, E. Wallin, I. Simon, G. Von Heijne, A. Elofsson, Prediction of transmembrane alpha-helices in procariotic membrane proteins: the dense alignment surface method, Protein Eng. 10 (1997) 673–676.
[142] A. Krogh, B. Larsson, G. von Heijne, E.L.L. Sonnhammer, Predicting transmembrane protein topology with a hidden Markov model: application to complete genomes, J. Mol. Biol. 305 (2001) 567–580.
[143] G. von Heijne, Membrane protein structure prediction. Hydrophobicity analysis and the positive inside rule, J. Mol. Biol. 225 (1992) 487–494.
[144] T. Hirokawa, S. Boon-Chieng, S. Mitaku, SOSUI: classification and secondary structure prediction system for membrane proteins, Bioinformatics 14 (1998) 378–379.
[145] G.E. Tusnády, I. Simon, The HMMTOP transmembrane topology prediction server, Bioinformatics 17 (2001) 849–850.
[146] A. Drozdetskiy, C. Cole, J. Procter, G.J. Barton, JPred4: a protein secondary structure prediction server, Nucleic Acids Res. (2015) ahead of print.
[147] B.P. Rost, P. Fariselli, R. Casadio, Topology prediction for helical transmembrane proteins at 86% accuracy, Protein Sci. 5 (1996) 1704–1718.